Passive RF Self-Localization of UAVs Using Signals of Opportunity: A Survey and Evaluation Study

Jort Kuipers[1]

Supervisor(s): Arash Asadi[1]**, Florian Kosterhon**[1]

[1]EEMCS, Delft University of Technology, The Netherlands

A Thesis Submitted to EEMCS Faculty Delft University of Technology,
In Partial Fulfilment of the Requirements
For the Bachelor of Computer Science and Engineering
June 21, 2026

Name of the student: Jort Kuipers
Final project course: CSE3000 Research Project
Thesis committee: Arash Asadi, Florian Kosterhon, Georgios Iosifidis

Abstract—
This work surveys and evaluates passive RF-based Signals of Opportunity (SoOP) for UAV self-localization in GNSS-denied environments. We review Time Difference of Arrival (TDoA), Angle of Arrival (AoA), Doppler shift, and Received Signal Strength Indicator (RSSI) measurement techniques, together with the state estimation frameworks used to process them. To evaluate these trade-offs in practice, a MATLAB simulation framework is developed using ray-traced urban channel models for TU Delft and Chicago, and a free-space open-field model. Three Extended Kalman Filter variants are compared across these environments: TDoA-only, RSSI-only, and fused TDoA+RSSI. Results show that TDoA consistently outperforms RSSI in all scenarios, while the fused filter yields improvements of up to 55% over TDoA alone in challenging NLOS configurations. The dominant factor governing localization accuracy is transmitter geometry and density rather than propagation model fidelity, and hybrid approaches are most beneficial precisely when single-modality observability is poor.

Index Terms—**signals of opportunity, UAV localization, GNSS-denied, passive RF, TDoA, Doppler, RSSI, AoA, Survey, Simulation**

I. Introduction

GLOBAL Navigation Satellite Systems (GNSSs) are fundamental to modern positioning and navigation, including Unmanned Aerial Vehicles (UAVs). Their widespread adoption stems from global coverage, low operational cost, and meter-level positioning accuracy. However, GNSS signals are inherently weak at the receiver and therefore highly susceptible to intentional interference, such as jamming and spoofing, which can degrade or completely deny localization.

The growing accessibility of low-cost GNSS jammers through online marketplaces further exacerbates this problem [1]. As UAVs continue to be deployed in safety-critical and autonomous applications, reliance on GNSS alone becomes increasingly problematic. Consequently, robust alternative localization techniques that can operate under GNSS-denied or GNSS-degraded conditions are receiving substantial research attention.

Signals of Opportunity (SoOP) have emerged as a promising alternative [1], exploiting existing ambient radio frequency (RF) transmissions; including cellular [2], Wi-Fi [3], and broadcast signals [4], without requiring dedicated positioning infrastructure. However, because these signals were not designed for navigation, SoOP localization introduces several challenges, including unknown transmission timing, limited synchronization between transmitters, and strong sensitivity to environmental effects. Some approaches also rely on prior environmental knowledge such as radio maps or fingerprinting databases [5].

Localization using SoOP can be achieved through several measurement modalities, including Time Difference of Arrival (TDoA) [6], Doppler shift [7], and Received Signal Strength Indicator (RSSI) measurements [3]. Recent advances in Radio SLAM further enable radio map construction without requiring pre-existing datasets [8].

Nevertheless, each localization modality presents its own limitations. TDoA-based methods often require synchronization between transmitters or receivers, Doppler relies on relative motion and accurate reference frequencies, and RSSI-based techniques are highly susceptible to multipath propagation and shadowing effects.

This work reviews the practicality and effectiveness of different SoOP sources for UAV self-localization under GNSS-denied conditions. Throughout this survey, we focus specifically on passive RF localization approaches, where the UAV does not transmit signals itself. After surveying the most common measurement and state estimation techniques, two measurement techniques will be simulated to show how they react to changes in geometry and environment.

a) Contributions: The main contributions of this work are summarized as follows:

- A structured overview of passive RF-based SoOP localization techniques for UAVs, categorizing measurement modalities (TDoA, AoA, Doppler, RSSI) and state estimation frameworks across the recent literature.
- A MATLAB simulation framework for evaluating SoOP-based UAV localization, incorporating free-space propagation for open-field scenarios and ray-traced urban channel models for real building geometries at TU Delft and Chicago.
- A quantitative comparison of TDoA-only, RSSI-only, and fused TDoA+RSSI Extended Kalman Filter variants, showing that fusion improves positioning accuracy by up to 55% over TDoA alone in NLOS-heavy urban configurations.
- An empirical analysis showing that transmitter geometry and spatial density are the dominant factors governing localization accuracy across all tested environments.

b) Paper Structure: The remainder of this paper is organized as follows. Section II describes the system background and assumptions. Section III covers the measurement modalities used in SoOP-based localization. Section IV discusses location estimation and filtering frameworks. Section V evaluates two different measurement techniques via a simulation, and shows the setup and approaches evaluated. Section VI presents results from the evaluation simulation, followed by discussion in section VII and conclusion in section VIII. Lastly, a Responsible Research section is included in section IX

II. Problem Formulation

Before examining specific localization techniques, it is necessary to define the underlying system model and measurement framework. In GNSS-denied environments, SoOP provide an alternative source of navigation information that can be exploited for state estimation. This section gives an introduction to SoOP and explains the UAV model and assumptions used throughout the survey.

A. Signals of Opportunity

SoOP are ambient radio frequency transmissions that exist independently of any navigation purpose. Relevant sources include terrestrial infrastructure such as LTE and 5G base stations, Wi-Fi access points, and FM broadcast transmitters, as well as Low Earth Orbit (LEO) satellite constellations such

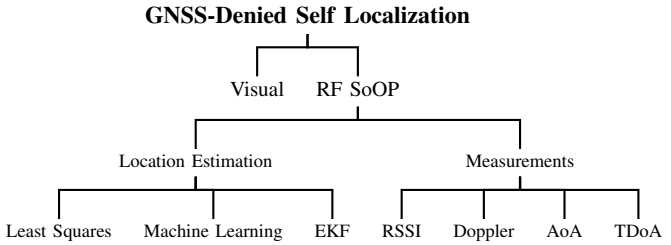

Fig. 1: Overview of Localization methods for UAV navigation.

as Iridium NEXT, Orbcomm, and Starlink. Terrestrial sources offer dense, fixed coverage in urban environments but are subject to strong multipath at low altitudes. LEO satellites provide wide-area coverage and produce strong Doppler signatures owing to their high orbital velocities [9], but their signals were designed for communication rather than ranging.

Because SoOP transmitters lack dedicated ranging codes and tight timing discipline, localization relies on extracting implicit geometric information from available signal properties: propagation time differences, frequency shifts, received power, or wavefront angle.

B. Model Assumptions

Platform. The localization platform is a single UAV under realistic resource and environmental constraints. Compared to ground vehicles or static receivers, UAV localization presents distinct challenges: limited payload and onboard computation, highly dynamic 3D motion, and real-time processing requirements. Cooperative and swarm-based approaches are discussed where relevant, but the primary focus remains on the single-agent case.

Passive reception. The UAV receives ambient SoOP transmissions without transmitting, removing the need for spectrum access, increasing scalability, and avoiding position disclosure.

Transmitter knowledge. Transmitter positions are assumed to be known or accessible from public databases (e.g., base station registries or satellite ephemerides). Works that relax this assumption, such as Radio SLAM or Differential Time Delay approaches, are identified explicitly.

Environment. Both outdoor and indoor scenarios are considered, with primary focus on outdoor localization relevant to long-range UAV navigation. Indoor environments are included due to growing use in humanitarian, industrial, and search-and-rescue missions.

State vector. The quantity to be estimated is at minimum the UAV's 3D position with its error.

III. Overview of Measurement Techniques

In this section, the available literature is categorized in terms of their measurement techniques. A brief overview of all different techniques can be found in Table I.

A. TDoA

The largest body of work on SoOP-based self-localization relies on TDoA. TDoA operates by measuring the difference in signal arrival times from multiple transmitters. Since radio signals propagate at the speed of light, the measured time difference directly corresponds to a difference in propagation distance between the UAV and two transmitters. For a pair of transmitters, the measured TDoA constrains the UAV position to a hyperbola in 2D space (or a hyperboloid in 3D), where all points satisfy a constant distance difference to the two transmitters. By combining TDoA measurements from multiple transmitter pairs, the UAV can estimate its own position through multilateration.

A key advantage of TDoA is that it eliminates the need for absolute clock synchronization between the receiver and transmitter. This is important because even very small clock differences, translate directly into large ranging errors due to the high propagation speed of radio signals. Instead, TDoA only requires synchronization among either the transmitters or the receivers (e.g. in swarm scenarios), which is generally more practical to achieve.

Several papers study the theoretical performance limits: Elgammal et al. [4] derive the Cramér-Rao Lower Bound (CRLB) for TDoA-based UAV localization with imperfect receiver synchronization, using analog TV (PAL) as the SoOP. Coluccia et al. [11] analyze positioning from SoOP in fully asynchronous settings, using the help of other GPS-enabled mobile terminals. Another useful measurement is the Differential Time Delay (DTD), where a single receiver observes the delay between the line-of-sight signal and its backscatter. Zhang and Ho [20] show that DTD-based localization can be possible without the knowledge of transmitter position or receiver synchronization, and can be just as accurate as TDoA. However, this work assumes receiver to be in a static position. They proposed a combined DTD + TDoA location estimator nearing the CRLB. For multi-source scenarios, Jamali-Rad and Leus [21] propose a sparsity-aware approach that jointly estimates the number of sources and their positions from TDoA measurements using fingerprinting, reducing computational load. In the 5G domain, Dureppagari et al. [22] exploit uplink Sounding Reference Signals (SRS) to position UAVs indoors with an Uplink TDoA (UTDOA) (indoor) framework using UAV anchors and SRS signals with CRLB derivation. Maul et al. [10] addresses the synchronization problem directly

TABLE I: Comparison of SoOP Localization Techniques

Technique	Accuracy	Scalability	Advantages / Limitations
TDoA [4], [10], [11]	Sub-m to tens of m	High	**Adv.:** Passive, infrastructure-light. **Lim.:** Requires synchronization; sensitive to NLOS/multipath
AoA [2], [12]–[14]	Sub-m to few m	Medium	**Adv.:** Geometry-friendly. **Lim.:** Requires antenna arrays; multipath-sensitive
Doppler [7], [15], [16]	Metres to tens of m	Medium	**Adv.:** No synchronization needed. **Lim.:** Requires fast-moving transmitters
RSSI [17], [18]	Low	Low	**Adv.:** Simple, low-cost hardware. **Lim.:** Environment-sensitive; poor outdoor accuracy
Hybrid [2], [14], [19], [20]	Best overall	High	**Adv.:** Combines complementary methods. **Lim.:** Increased system complexity

using a hardware off the shelve architecture. Achieving sub-nanosecond clock alignment between spatially separated SDR receivers using SoOP cross-correlation, nearing the theoretical limit. Lastly, de Sousa et al. [23] use machine learning to improve localization accuracy by training Random Forest and Gradient boosting Machine Learning algorithms on simulations, and use that to estimate the real life scenario.

TDoA remains one of the most mature and accurate SoOP-based localization techniques. The reviewed literature demonstrates that considerable progress has been made in addressing its traditional limitations, particularly synchronization requirements and dependence on known transmitter locations. While many of these solutions introduce additional hardware, infrastructure, or computational complexity, they show that these challenges are increasingly manageable in practical deployments.

B. AoA

Angle of Arrival (AoA) estimates signal direction by measuring the phase, time, or amplitude differences between multiple spatially separated antenna elements. Using the known positions of multiple transmitters, the receiver can estimate its own position through triangulation by intersecting the measured arrival angles. In two-dimensional space, each AoA measurement constrains the receiver position to a line extending from the transmitter along the estimated angle. Combining multiple AoA measurements from different transmitters allows the receiver position to be determined.

Like TDoA, AoA can achieve very high localization accuracy and often provides sub-meter to few-meter positioning performance [13]. A key advantage of AoA is that, unlike TDoA, it does not require synchronization between transmitters or receivers. However, AoA generally requires antenna arrays consisting of multiple spatially separated elements, increasing hardware complexity and size. These requirements can make AoA more difficult to implement on UAV platforms with limited payload capacity.

Despite these challenges, AoA has been successfully applied in a variety of localization scenarios. Although many studies focus on ground vehicles rather than UAVs, the underlying estimation methods remain relevant. For example; Fascista et al. [13] determine vehicle position using AoA measurements of beacon packets transmitted by roadside units (RSUs). These measurements are combined with a Weighted Least Squares (WLS) algorithm. Shao et al. [12] introduce auxiliary-variable based estimators to reduce estimation bias while maintaining low computational complexity compared to iterative maximum likelihood methods.

An example of UAV based localization using AoA is by McGuire et al. [24]. In this paper, the location of the UAV is estimated with the help of stationary and moving beacons at known positions. In combination with an Unscented Kalman Filter (UKF) with an informative path planning (IPP) algorithm, approaching the CRLB under optimal trajectories.

SLAM algorithms can also be implemented utilizing AoA and Direction of arrival (DoA) measurements, as seen in the review by Bisma et al. [8] with a focus on mm-wave enabled localization and SLAM methods.

Another limitation of AoA is its sensitivity to multipath propagation. Unlike TDoA, where multipath typically introduces timing biases, reflected signals in AoA systems can directly corrupt angle estimates, leading to large position errors. Combined with the need for antenna arrays, this remains a key obstacle for deployment on small UAV platforms.

Despite these limitations, AoA can achieve high localization accuracy without strict synchronization requirements or extensive transmitter-side infrastructure. Continued advances in antenna design and signal processing are improving its practicality for UAV applications, particularly in beacon-assisted localization and SLAM systems.

C. Doppler

Doppler-based localization exploits frequency shifts caused by relative motion between transmitter and receiver, providing constraints on the radial velocity component and enabling position estimation when transmitter trajectories are known. Low Earth Orbit (LEO) satellites are particularly suitable due to their high orbital velocities and predictable motion, making Doppler measurements strong and informative. In recent years, LEO satellite systems have therefore become a major focus of Doppler-based localization research. An overview of this field is provided by Liu et al. [9], who survey the full pipeline of LEO SoOP positioning from constellation properties to fusion strategies.

A practical multi-constellation framework is proposed by Orabi et al. [15], where Doppler frequency measurements are extracted from both Orbcomm and Iridium NEXT satellites, using a receiver architecture that handles both time division (TDMA) and frequency division multiple access (FDMA) signals. An Extended Kalman Filter (EKF) fuses these measurements to estimate a stationary receiver's position.

Kozhaya and Kassas [16] propose a blind Doppler spectral approach for Starlink LEO satellites, where neither the satellite location nor signal structure needs to be known a priori. A frequency-domain blind Doppler discriminator is derived analytically, followed by a Kalman filter tracking stage. Doppler measurements from six Starlink satellites are merged by minimizing a nonlinear least-squares cost function, yielding a final 2D horizontal position error of 4.3 m.

A limitation in Doppler-based LEO positioning is that the received signal often lacks orbit information and signal emission time, introducing significant errors. Zhao et al. [7] address the lack of emission time information via a Differential Doppler (DD) framework with a Maximum Likelihood Estimation (MLE)-based Signal Emission Time Estimation (SETE) algorithm.

In summary, Doppler-based localization uses frequency shifts caused by relative motion to estimate position or velocity. It is particularly effective with LEO satellite signals, where high orbital speeds provide strong Doppler measurements. Overall, Doppler-based methods are a promising SoOP localization technique, especially in satellite-rich environments.

D. RSSI

Another possible measurement source for self-localization is the Received Signal Strength Indicator (RSSI). RSSI measures

the received power of a signal at the receiver. Since radio signals attenuate as they propagate through space, the received signal strength can be related to the distance between the transmitter and receiver through a propagation model. By estimating the distance to multiple transmitters with known positions, the receiver can estimate its own position using trilateration.

However, RSSI is not often used for accurate self-localization. This is mainly due to its high sensitivity to noise, multipath propagation, antenna orientation, and environmental geometry. As a result, RSSI-based localization is often inaccurate when directly estimating receiver position. Instead, RSSI is more commonly used for fingerprinting purposes.

Fingerprinting is the process of constructing a database, containing previously measured signal characteristics at known locations within an environment. During operation, the receiver measures the currently observed RSSI values from surrounding transmitters and compares these measurements against the stored fingerprints. The estimated position is then determined as the location whose stored signal signature best matches the observed measurements. The accuracy is highly dependent on the density of transmitters within an area and the quality of the stored fingerprints.

Nonetheless, direct RSSI-based localization is still feasible. Jondhale et al. [18] present a range of RSSI-based approaches, including distance-based trilateration and wireless sensor network (WSN) tracking methods, along with their respective system designs and limitations.

Moreover, Abouzar et al. [17] propose a distributed Bayesian localization algorithm to solve the approximate inference problem, based on message passing. Though this work is mainly based for agricultural purposes, we do believe the mentioned methods and algorithms could be relevant in the UAV localization field. If not for just giving some information about how to localize using RSSI.

A prerequisite for fingerprinting-based systems is the availability of high-quality, representative datasets. Klus et al. [3] address this by introducing TUJI1, a densely sampled Wi-Fi fingerprinting dataset collected across five different commercial devices in a fine-grained indoor grid. The dataset provides matched RSSI measurements with corresponding ground-truth coordinates, split into training and testing subsets. Mondal [5] extends the fingerprinting concept to outdoor environments, investigating radio frequency fingerprinting for user equipment localization in outdoor scenarios, where the radio map construction and matching problem differs from the indoor case due to sparser infrastructure and bigger propagation effects.

In summary, RSSI-based localization estimates distance from received signal power and is simple to implement but generally inaccurate in practice due to strong sensitivity to multipath, shadowing, and environmental effects. Consequently, it is more commonly used in fingerprinting approaches, where pre-collected radio maps are matched against observed measurements. While fingerprinting can improve accuracy under controlled conditions, it requires large amounts of data and degrades when the environment changes. Overall, RSSI offers low-complexity localization at the cost of limited robustness and accuracy.

E. Hybrid Approaches

Several works combine two or more measurement or estimation techniques to compensate for the individual weaknesses of each. These hybrid systems generally outperform any single-modality approach, at the cost of increased system complexity and/or costs.

He and So [19] combine TDOA and RSS fingerprinting for LTE indoor positioning: a coarse TDOA estimate via SRS is refined by a deep neural network performing fingerprint matching. The resulting system achieves sub-meter level positioning accuracy, showing that TDOA and fingerprinting together can compensate for the individual weaknesses of each method.

Moreover, Shamaei et al. [14] use 3D Matrix Pencil (MP) to LTE reference signals for joint TOA/DOA estimation, combined with an EKF for position. achieving a final positioning error of 0.55 m after 15 s in a real-world conditions. Shamaei et al. [2] later extended this with a two-stage receiver: A 3-D MP-based stage for rough TOA/DOA initialization, followed by a tracking loop that continuously refines and tracks TOA and DOA changes over time.

Zhang and Ho [20] propose a joint DTD and TDOA estimator that combines Differential Time Delay measurements, which do not require transmitter position knowledge, with conventional TDOA to approach the CRLB without synchronization between the receiver and transmitters. The combination of the two measurement types allows for greater accuracy: DTD provides positioning capability when transmitter positions are unknown, while TDOA contributes tighter geometric constraints when multiple synchronized transmitters are available.

IV. Overview of Location Estimation Techniques

This section builds on section III, which introduced the main measurement modalities used in SoOP-based localization, such as TDoA, AoA, Doppler, and RSSI. While those techniques describe what is being measured, this section focuses on how these heterogeneous and often noisy measurements are processed to obtain a position estimate. In particular, it reviews the main classes of estimation methods used in the literature, including recursive state-space filtering, optimization-based solvers, spectral parameter estimation techniques, and data-driven approaches.

A. Kalman-Based Filters

The Extended Kalman Filter (EKF) is the most widely used estimator in SoOP localization, recursively combining noisy measurements with a dynamic motion model at low computational cost.

Orabi et al. [15] employ an EKF to fuse Doppler frequency measurements from Orbcomm and Iridium NEXT LEO satellites, achieving 22.7 m error. Shamaei et al. [14] combine a MP-based TOA/DOA extraction stage with an EKF for continuous position and clock bias estimation, achieving a final error of 0.55 m after 15 s in a real-world LTE environment. The Radio SLAM approach of [1] also relies on an EKF to propagate and update the receiver state under LTE signals in a

GPS-jammed environment, achieving 32 m RMSE over a 5 km trajectory.

For scenarios with stronger nonlinearity, the Unscented Kalman Filter (UKF) offers improved accuracy by propagating a set of deterministically chosen sigma points through the nonlinear measurement model. McGuire et al. [24] adopt a UKF in combination with an informative path planning algorithm for AoA-based UAV localization, approaching the CRLB under optimal trajectories.

Kozhaya and Kassas [16] employ a standard linear Kalman filter as the tracking stage in their blind Doppler framework for Starlink satellites, preceded by a frequency-domain discriminator for Doppler extraction.

B. Least Squares Methods

Least squares (LS) based estimators are common in SoOP localization due to their simplicity, closed-form solutions, and near-CRLB performance under mild noise assumptions.

Coluccia et al. [11] apply a cooperative WLS estimator for TDOA-based positioning in fully asynchronous settings, approaching the CRLB across a range of SNR conditions. Fascista et al. [13] similarly use WLS to fuse AoA measurements from roadside units for vehicle localization, outperforming GPS accuracy at ranges below 134 m.

Zhang and Ho [20] formulate a joint DTD/TDOA estimator that approaches the CRLB without requiring knowledge of the transmitter position or receiver synchronization. Kozhaya and Kassas [16] finalize their Starlink Doppler positioning pipeline with a Nonlinear Least Squares (NLS) cost function minimization over multiple satellite measurements, yielding a 2D horizontal position error of 4.3 m.

Dureppagari et al. [22] propose an Iterative Parallel Projection Method (IPPM) as a lower-complexity alternative to NLS for 5G UTDOA positioning using UAV anchors, achieving near-CRLB performance with reduced computational load.

C. Spectral and Subspace Methods

The Matrix Pencil (MP) method is a high-resolution spectral technique for estimating signal parameters such as time-of-arrival and angle-of-arrival from multi-antenna array data without requiring iterative optimization.

Shamaei et al. [14] apply a 3D Matrix Pencil to LTE reference signals for joint TOA and DOA extraction, which are subsequently fed into an EKF for position estimation, achieving sub-meter accuracy in real-world experiments. The same group extended this in [2] by using the MP as an acquisition stage to initialize a continuous tracking loop, reducing the standard deviation of TOA estimation by 93%.

Kozhaya and Kassas [16] take a complementary spectral approach, deriving a blind frequency-domain Doppler discriminator for Starlink signals without any a priori knowledge of the satellite's ephemeris or signal structure.

D. Machine Learning

Data-driven methods have begun to appear in SoOP localization, particularly where the relationship between observables and position is difficult to model analytically.

De Sousa et al. [23] train Random Forest and Gradient Boosting regressors on simulated TDoA data and apply the trained models to real-world scenarios. The approach achieves a mean distance error of 1.38 m in simulation, with approximately 46% of real-world predictions falling within 75 m, demonstrating the sim-to-real transfer challenge inherent to this approach.

He and So [19] integrate a deep neural network into a hybrid TDOA/RSS pipeline for LTE indoor positioning. The network performs fingerprint matching within a restricted subregion, achieving sub-meter positioning accuracy while compensating for NLOS and multipath effects that degrade pure TDOA estimates.

E. Bayesian and Sparsity-Aware Methods

Bayesian estimators offer a principled framework for handling measurement uncertainty and prior knowledge, and are particularly useful in distributed or sparse measurement scenarios.

Abouzar et al. [17] propose a distributed Bayesian localization algorithm based on message passing over a wireless sensor network for RSSI-based positioning.

Jamali-Rad and Leus [21] take a sparsity-aware approach, jointly estimating the number of active SoOP sources and their positions from TDoA measurements. By exploiting the sparse structure of the source distribution, the method reduces both computational load and the need for prior knowledge about source count.

F. Maximum Likelihood and Closed-Form Estimators

MLE provides statistically optimal estimates when the noise model is well characterized. Zhao et al. [7] apply MLE through their SETE algorithm within a Differential Doppler framework, reducing 3-D positioning error by 86.3%.

For constrained computational resources, closed-form algebraic estimators offer near-optimal accuracy without iterative solvers: Shao et al. [12] introduce an auxiliary-variable based closed-form AoA estimator that reduces estimation bias while maintaining computational efficiency.

In summary, the choice of estimation method depends on the problem structure and available prior information. Kalman-based filters are well suited to real-time tracking with dynamic motion models, while least-squares methods remain popular for snapshot localization due to their simplicity and effectiveness under Gaussian noise. Spectral methods are commonly used to extract parameters such as TOA, DOA, and Doppler before subsequent estimation. Machine learning approaches can model complex nonlinear relationships but require substantial training data, whereas Bayesian and sparsity-aware methods are particularly effective when uncertainty or prior structural knowledge must be incorporated.

V. Evaluation

Having surveyed the available SoOP-based self-localization approaches, this section evaluates two representative measurement modalities, RSSI and TDoA, and their fusion, to illustrate the trade-offs identified in the taxonomy.

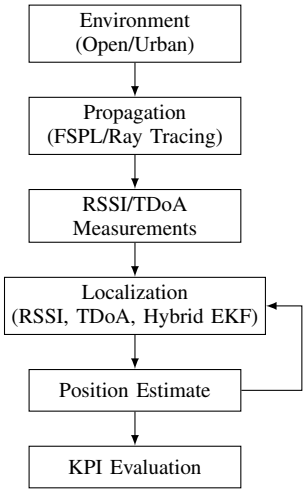

Fig. 2: Simulation workflow used for evaluating SoOP-based UAV self-localization methods.

A rough overview of the stages in the simulation can be found in Figure 2

A. Simulation Settings

1) Environments: Two contrasting scenarios are considered. The **open-field** scenario covers a 5000×5000 m area representative of Dutch rural farmland, with six randomly placed mast-mounted transmitters (heights 15–60 m, $P_{\text{tx}} = 63$ dBm, $f_c = 2.4$ GHz), using MATLAB's `fspl()` function [25] for propagation.

Two **urban** scenarios use real building geometry from OpenStreetMap: the TU Delft campus (7 transmitters) and the Chicago city center (8 transmitters), both positioned from a real cell-tower database [26], [27], both at $P_{\text{tx}} = 43$ dBm (20 W). Propagation is simulated with MATLAB's shooting-and-bouncing-ray (SBR) tracer [28]. NLOS and multipath are handled implicitly by the ray-tracer physics.

2) UAV Trajectories: In the open-field the UAV follows a sinusoidal 3D path across the full domain over $T = 200$ steps ($\Delta t = 1$ s). Both urban trajectories are defined in WGS-84 and converted to the local ENU frame over $T = 30$ steps ($\Delta t = 2$ s), but follow different ground tracks. Over TU Delft, the UAV flies a straight-line ground track with a sinusoidal lateral (East) oscillation superimposed (3 cycles, ± 45 m) at 34–50 m AGL, over the campus park. Over Chicago, the UAV instead follows a road-aligned route defined by six lat/lon waypoints along the city's street grid, with altitude oscillating between roughly 30–50 m AGL.

3) Measurements: At each time step k the UAV collects two measurement types, RSSI and TDoA. In the **open-field** scenario both are generated analytically from the true Euclidean distance d_i to each transmitter:

$$P_{\text{rx},i} = P_{\text{tx}} - \text{FSPL}(d_i, \lambda) + \xi_i, \quad \xi_i \sim \mathcal{N}(0, \sigma_{\text{sf}}^2), \tag{1}$$

$$\tau_i = \frac{d_i - d_1}{c} + \nu_i, \quad \nu_i \sim \mathcal{N}(0, \sigma_\tau^2), \quad i = 2, \ldots, N_{\text{tx}}, \tag{2}$$

with $\sigma_\tau = 10$ ns.

In the **urban** scenarios both quantities come directly from the SBR ray tracer at each step, by placing a receiver at the UAV's true lat/lon/altitude and calling `raytrace()` against every transmitter. If no path is returned for a transmitter, its measurements are marked unavailable for that step. Otherwise, time-of-arrival is taken from the first-arriving ray's geometric length (blended 30% toward the second-arriving ray's length where one exists, to soften abrupt dominant-path switches), converted to a delay and corrupted with hardware timing noise ($\sigma_\tau = 20$ ns); RSSI is obtained from `raypl()` [29] on every returned ray, combined as $\text{PL}_{\text{tot}} = -10 \log_{10} \sum_k 10^{-\text{PL}_k/10}$ to account for multipath, with shadow fading added afterward.

Because the EKF correction step requires a fixed-length measurement vector, unavailable entries are zero-filled with an artificially huge variance ($R = 10^8$), driving their Kalman gain to zero while keeping the vector length fixed at $N_{\text{tx}} - 1$ (TDoA) and N_{tx} (RSSI). Available TDoA entries pass an additional 3σ outlier gate against the filter's prediction, inflating that entry's variance $5\times$ on excessive residuals to limit the influence of mismatched multipath without discarding the entry. Key parameters are summarized in Table V.

4) Performance Metrics: Performance is reported as 3D RMSE against ground-truth UAV position. Open-field results use RMSE over $N_{\text{MC}} = 50$ Monte Carlo trials. Urban results are single deterministic runs, since ray tracing is too expensive for large-scale repetition.

B. Approaches

Three EKF variants are compared under identical conditions: TDoA-only, RSSI-only, and Fused (TDoA + RSSI). Using the same estimator throughout isolates the contribution of each measurement type.

All three filters are initialized from the same randomly perturbed starting position (horizontal perturbation $\sim \mathcal{N}(0, 5^2)$ m, vertical $\sim \mathcal{N}(0, 2^2)$ m, zero initial velocity) and run over identical measurement sequences.

1) State and Motion Model: The EKF state is $\mathbf{x} = [x\ y\ z\ \dot{x}\ \dot{y}\ \dot{z}]^\top \in \mathbb{R}^6$ in the local ENU frame. A constant-velocity model is assumed:

$$\mathbf{x}_{k+1} = \mathbf{F}\,\mathbf{x}_k, \qquad \mathbf{F} = \begin{bmatrix} \mathbf{I}_3 & \Delta t\,\mathbf{I}_3 \\ \mathbf{0}_3 & \mathbf{I}_3 \end{bmatrix}. \tag{3}$$

Process noise is diagonal; open-field uses $\mathbf{Q}_{\text{open}} = \text{diag}(5, 5, 5, 1, 1, 1)$ and both urban environments use $\mathbf{Q}_{\text{urban}} = \text{diag}(5, 5, 0.5, 1, 1, 0.1)$, reflecting greater lateral than vertical variability in the state and in the assumed UAV dynamics.

2) Measurement Functions in EKF: The RSSI prediction uses a log-distance path-loss model with a deterministic bias term:

$$\hat{P}_{\text{rx},i}(\mathbf{x}) = P_{\text{tx}} - \text{PL}_0 - 10\,n \log_{10}(d_i(\mathbf{x})) + b(d_i(\mathbf{x})). \tag{4}$$

with $(\text{PL}_0, n) = (40\,\text{dB}, 3.2)$ for TU Delft and $(40\,\text{dB}, 3.8)$ for Chicago. Ray tracing is not used inside the filter due to its cost and non-differentiability; the resulting model mismatch is absorbed by an enlarged, distance-dependent measurement covariance rather than a single fixed value (see below).

TABLE II: Localization RMSE in the Urban Chicago environment for different transmitter configurations and reflection orders.

Configuration	TDoA	RSSI	Fused
2 Reflections			
TX2 at 164 m (LOS)	131.2 m	154.7 m	110.1 m
TX2 at 44 m (NLOS)	127.5 m	174.5 m	111.5 m
8 Reflections			
TX2 at 164 m (LOS)	130.7 m	168.8 m	118.3 m
TX2 at 44 m (NLOS)	135.2 m	176.9 m	116.5 m
16 Reflections			
TX2 at 164 m (LOS)	135.3 m	163.7 m	113.7 m
TX2 at 44 m (NLOS)	123.1 m	172.6 m	129.5 m
20 TXs spread along the trajectory	123.0 m	131.7 m	95.1 m

The TDoA measurement model uses hyperbolic range-difference geometry with the same dynamically selected reference transmitter as in measurement generation:

$$\hat{\tau}_i(\mathbf{x}) = \frac{d_i(\mathbf{x}) - d_{\mathrm{ref}}(\mathbf{x})}{c}, \qquad i \in \{1, \ldots, N_{\mathrm{tx}}\} \setminus \{\mathrm{ref}\}. \quad (5)$$

Its covariance uses a fixed urban baseline variance σ^2_{NLOS}, augmented by innovation-based gating: residuals exceeding $\gamma\sigma$ are flagged as outliers and their variance inflated, identically for TDoA-only and the TDoA component of the fused filter.

For the RSSI-only filter, the covariance is a constant shadow-fading variance σ^2_{sf} for available links, with unavailable links given effectively infinite variance:

In the fused filter, RSSI covariance instead uses a distance-based LOS-probability surrogate, assigning higher uncertainty to distant (more likely NLOS) transmitters.

The fused observation vector stacks both modalities:

$$\mathbf{z}_k = \begin{bmatrix} \boldsymbol{\tau}_k \\ \mathbf{P}_{\mathrm{rx},k} \end{bmatrix} \in \mathbb{R}^{2N_{\mathrm{tx}}-1}. \quad (6)$$

with block-diagonal covariance

$$\mathbf{R}_{\mathrm{fused}} = \mathrm{blkdiag}\big(w_\tau \mathbf{R}_\tau,\ w_{\mathrm{RSSI}} \mathbf{R}_{\mathrm{RSSI}}\big), \quad (7)$$

with $w_\tau = 1$ and $w_{\mathrm{RSSI}} = 0.4$, reflecting the higher expected reliability of TDoA under the assumed urban propagation conditions.

VI. Experiments and Results

A. Chicago

This subsection evaluates localization performance in the urban Chicago ray-tracing scenario, focusing on how transmitter geometry and transmitter density shape the relative strengths of TDoA, RSSI, and the fused filter.

To isolate the effect of line-of-sight availability, a single transmitter (TX2) was placed in two configurations: a rooftop position at approximately 164 m altitude with a clear line of sight to most of the UAV trajectory, and a lower position at approximately 44 m altitude, behind nearby buildings to create a NLOS condition for that link. Both transmitters are placed at real Chicago transmitter locations [27]. Table II reports the resulting 3D RMSE. Figure 3 shows the UAV trajectory and its position estimates, as well as the transmitter locations.

TABLE III: Urban TU Delft localization RMSE.

Configuration	TDoA	RSSI	Fused
2 Reflections			
4 TX at NLOS handpicked locations	134.2 m	156.2 m	59.9 m
7 Real transmitters	46.5 m	196.7 m	52.5 m
4 Reflections			
4 TX at NLOS handpicked locations	134.2 m	156.2 m	59.9 m
7 Real transmitters	45.3 m	147.5 m	42.0 m
8 Reflections			
4 TX at NLOS handpicked locations	134.2 m	156.2 m	59.9 m
16 Reflections			
7 Real transmitters	45.4 m	147.5 m	41.9 m

Overall, the results show that RSSI-only localization is consistently the weakest, with errors in the range of 154.7–176.9 m, corresponding to a degradation of up to $\sim$30% relative to TDoA in the best case. This indicates limited geometric observability of RSSI in the urban multipath setting. The fused EKF often times is the best out of the modalities. It is clear that some of the weaknesses of TDoA are compensated by RSSI and vice versa. Leading to a 22.68% improvement compared to TDoA, and a 27.79% improvement compared to RSSI, in the 20 Transmitter case, which is the most realistic. Moreover, we see that when changing the transmitter location to a NLOS position, decreases RSSI accuracy, with TDoA staying roughly the same or even improving, interestingly enough. It also shows that changing the amount of reflections has more impact on the NLOS case, compared to the LOS case. Nonetheless, we still see that Fused is the most accurate approach, with very little deviance in a NLOS or LOS, showing that Fused is the least vulnerable to LOS changes Finally, increasing transmitter diversity yields the strongest gain: using 20 transmitters reduces fused RMSE to 95.1 m, an improvement of $\sim$14% compared to the best 8 transmitter configuration (110.1 m). This shows that spatial diversity is most important in localization accuracy.

B. TU Delft

The TU Delft scenario uses the 7 real-world cell-tower positions described in Section V-A, as well as 4 handpicked positions; some of which having less LOS to the UAV, evaluated along the campus park trajectory. Table III reports the resulting RMSE. Figure 4 shows the UAV trajectory and its position estimates, as well as the transmitter locations.

RSSI-only localization is again the weakest modality, with errors of 147.5–196.7 m, up to $\sim$76% worse than TDoA in the best case. The fused EKF performs best overall, though its benefit depends on transmitter geometry: with the 7 real transmitters, TDoA alone is already accurate, so fusion adds only a modest $\sim$7–8% improvement (e.g., $45.3\,\mathrm{m} \rightarrow 42.0\,\mathrm{m}$), and at 2 reflections fusion even underperforms TDoA-only (46.5 m vs. 52.5 m), suggesting RSSI can inject noise when TDoA is already near-optimal. For the 4 TX NLOS handpicked configuration, fusion is far more impactful, improving on TDoA by 55.4% and on RSSI by 61.7% ($134.2\,\mathrm{m}$, $156.2\,\mathrm{m} \rightarrow 59.9\,\mathrm{m}$), with identical RMSE across all tested reflection orders, indicating that performance here is governed by transmitter

TABLE IV: Open Field localization RMSE using randomly distributed transmitters.

Configuration	TDoA	RSSI	Fused
3 Transmitters,	1206.0 m	1192.0 m	627.6 m
4 Transmitters	148.2 m	1039.9 m	146.4 m
5 Transmitters	15.0 m	832.9 m	15.0 m
6 Transmitters	15.3 m	1030.4 m	15.3 m
9 Transmitters	7.6 m	819.0 m	7.6 m
Area size 10000×10000 m:			
6 Transmitters	22.9 m	2210.6 m	22.9 m

placement and link availability. Comparing configurations, the 7-transmitter layout gives much better TDoA accuracy.

C. Open Field

This subsection reports open-field localization performance for the TDoA-only, RSSI-only, and fused EKF variants under the free-space propagation model defined in Section V-A, evaluated over $N_{\mathrm{MC}} = 50$ Monte Carlo trials.

The results show a strong dependence on transmitter density for TDoA-based localization, with performance improving significantly as the number of transmitters increases. RSSI-based localization remains inaccurate across all configurations, with errors exceeding 1000 m RMSE, indicating poor observability under the open-field scenario. The fused EKF closely tracks the TDoA-only performance in most cases, indicating that RSSI contributes negligible additional information in this scenario. An exception is observed for the 3-transmitter case, where a noticeable improvement over TDoA-only is obtained, mainly due to the poor conditioning of the TDoA solution in this configuration. We also observe a slight increase in RMSE when moving from 5 to 6 transmitters. This is likely due to the random transmitter placement resulting in a less favorable geometry, illustrating that performance depends not only on the number of transmitters but also on their spatial configuration.

Across all three environments, RSSI-only localization is consistently the weakest modality, ranging from moderately degraded in dense urban settings ($\sim$30–76% worse than TDoA) to effectively unusable in open field ($>$1000 m RMSE). TDoA-only performance, by contrast, is highly environment-dependent: it is near-optimal in open field given sufficient transmitter density (as low as 7.6 m), moderate in TU Delft with well-placed real transmitters (45 m), and substantially degraded under dense multipath and NLOS in Chicago (120–150 m).

The relative benefit of fusion scales inversely with TDoA quality. In open field, where TDoA is already highly accurate, fusion adds negligible improvement, as RSSI is effectively down-weighted by the filter. In Chicago and the TU Delft NLOS configuration, where TDoA alone is comparatively unreliable, fusion yields its largest gains ($\sim$23–62%), as RSSI compensates for TDoA's geometric weaknesses and vice versa. This pattern indicates that the fused EKF is most valuable precisely when single-modality observability is poor, and that transmitter density and geometry are the dominant factors governing localization accuracy.

VII. Discussion

The simulation results are broadly consistent with the findings from the literature review. TDoA provides the highest localization accuracy when transmitter geometry is favorable, but its performance degrades under sparse deployments and NLOS conditions. RSSI remains unusable for accurate standalone localization. As reported throughout the literature, combining complementary measurement modalities improves robustness, which is reflected in the fused EKF results. The benefits of fusion are most pronounced in challenging environments where TDoA performance deteriorates, while providing limited gains when TDoA measurements are already sufficiently accurate.

A limitation of this work is that the simulation considers only TDoA and RSSI, omitting Doppler and AoA. Of these, Doppler is arguably the more consequential omission going forward. The rapid growth of dense LEO constellations such as Starlink, combined with recent blind Doppler estimation methods that require no prior knowledge of signal structure or base stations, has greatly improved the accuracy of this technique. As satellite availability and signal density continue to increase, Doppler-based SoOP localization is likely to become one of the more practical and scalable options for UAV navigation, and its absence from the current simulation should be seen as a significant gap, motivating it as a priority for future extensions of this work.

VIII. Conclusion

This work presented a survey of passive RF-based signals of opportunity (SoOP) localization for UAV navigation in GNSS-denied environments, covering TDoA, AoA, Doppler, and RSSI measurements together with the state estimation frameworks used to process them. The literature review highlights that no single modality is universally optimal; rather, localization performance depends on the trade-off between accuracy, robustness, and implementation complexity, with hybrid approaches generally offering the best overall performance.

To complement the literature review, a MATLAB simulation framework was developed to evaluate TDoA-only, RSSI-only, and fused TDoA+RSSI EKF localization in both open-field and urban environments. Across all scenarios, TDoA consistently outperformed RSSI as a standalone modality, while the fused EKF achieved the best overall performance in challenging urban and NLOS conditions, improving localization accuracy by up to 55% compared to TDoA alone. The results further show that transmitter geometry and spatial density are the primary factors governing localization accuracy, often having a greater impact than the specific propagation model.

Future work should investigate Doppler-based localization using emerging LEO constellations, as well as transmitter-independent localization methods for moving UAVs. In addition, adaptive measurement-noise estimation techniques could further improve robustness under environmental variability and propagation model mismatch.

IX. Responsible Research

A. Reproduction

All simulations were conducted in MATLAB. The source code is publicly available on GitHub: https://github.com/lurt04/CSE3000-Research-Project-SoOP-UAV-Self-Localization-Simulation

Simulation experiments were performed on a Dell XPS 15 9520 laptop running Windows 11, featuring an Intel Core i7-12700H processor, an NVIDIA GeForce RTX 3050 Ti graphics card, 32 GB of DDR5 RAM, and a 1 TB M.2 SSD.

B. Dual-Use Considerations

SoOP-based navigation technology can improve safety and resilience for civilian UAV applications (search and rescue, package delivery). However, the same techniques could in principle enhance the navigational autonomy of adversarial UAVs. We note that the presented methods rely on existing civilian broadcast infrastructure and do not themselves introduce new RF emissions or exploit classified signals. All methods can be reproduced by without the need of classified information or infrastructure. All of this research can be reproduced by using already public information, which would not give any adversaries any extra advantage as compared to humanitarian UAVs.

C. Ethical Implications

A key ethical concern for any GNSS-denied localization system is the consequence of inaccurate or failed position estimates. An autonomous UAV that relies on a degraded or incorrect localization solution, for instance due to poor transmitter geometry or unmodeled NLOS propagation, may deviate from its intended trajectory, enter restricted or unsafe airspace, or collide with obstacles, structures, or people. This risk is particularly relevant in the urban and search-and-rescue scenarios that motivate SoOP-based navigation, where the environments are often inherently more hazardous and the localization errors observed in this work (on the order of tens to over a hundred meters in NLOS-heavy conditions) could be operationally significant. Because passive SoOP localization depends on uncontrolled, third-party signal sources, the system has no guarantee of consistent coverage or signal quality, making graceful degradation and reliable uncertainty estimation essential before such methods are deployed in safety-critical autonomous operation. Any real-world application should therefore be paired with safeguards such as fallback navigation modes, proximity sensors, conservative confidence thresholds, and human oversight, rather than full reliance on SoOP-based estimates alone.

D. AI Usage Statement

The following tasks used an AI assistant (Claude, Anthropic; ChatGPT, OpenAI) for LaTeX scaffolding, restructuring support, and iterative text refinement:

- Converted the original IJCAI-based template to the official IEEE Journal (`IEEEtran`) class.
- Restructured section files to match the required CSE3000 author instructions.
- Added cover-page block with Brightspace-required metadata.
- Replaced `unsrt/named` bibliography style with `IEEEtran` for correct IEEE numeric citations.
- Designed and refined table layouts for clarity and space efficiency in a two-column format.
- Iteratively shortened and improved technical descriptions in tables for conciseness and readability.
- Assisted in rephrasing and compressing methodological descriptions while preserving technical meaning.
- Assisted in sentence structure and clear writing.

All research content, scientific claims, interpretation of literature, and final narrative writing were authored by the student.

References

[1] Z. M. Kassas, J. Khalife, A. A. Abdallah, and C. Lee, "I am not afraid of the gps jammer: Resilient navigation via signals of opportunity in gps-denied environments," *IEEE Aerospace and Electronic Systems Magazine*, vol. 37, no. 7, pp. 4–19, 2022.

[2] K. Shamaei and Z. M. Kassas, "A joint toa and doa acquisition and tracking approach for positioning with lte signals," *IEEE Transactions on Signal Processing*, vol. 69, pp. 2689–2705, 2021.

[3] L. Klus, R. Klus, E. S. Lohan, J. Nurmi, C. Granell, M. Valkama, J. Talvitie, S. Casteleyn, and J. Torres-Sospedra, "Tuji1 dataset: Multi-device dataset for indoor localization with high measurement density," *Data in Brief*, vol. 54, p. 110356, 2024. [Online]. Available: https://www.sciencedirect.com/science/article/pii/S2352340924003251

[4] K. W. Elgammal, B. C. Turan, O. Bedir, H. Celebi, M. K. Qaraqe, and M. K. Ozdemir, "Theoretical limits of soop tdoa localization of unmanned systems with imperfect synchronization," in *2023 IEEE 28th International Workshop on Computer Aided Modeling and Design of Communication Links and Networks (CAMAD)*, 2023, pp. 158–163.

[5] R. U. Mondal, *Radio frequency fingerprinting for outdoor user equipment localization*. "University of Jyväskylä", 2017.

[6] C. Yan and H. Howard Fan, "Asynchronous differential tdoa for non-gps navigation using signals of opportunity," in *2008 IEEE International Conference on Acoustics, Speech and Signal Processing*, 2008, pp. 5312–5315.

[7] C. Zhao, H. Qin, N. Wu, and D. Wang, "Analysis of baseline impact on differential doppler positioning and performance improvement method for leo opportunistic navigation," *IEEE Transactions on Instrumentation and Measurement*, vol. 72, pp. 1–10, 2023.

[8] B. Amjad, Q. Z. Ahmed, P. I. Lazaridis, M. Hafeez, F. A. Khan, and Z. D. Zaharis, "Radio slam: A review on radio-based simultaneous localization and mapping," *IEEE Access*, vol. 11, pp. 9260–9278, 2023.

[9] P. Liu, H. Qin, J. Lu, R. Liu, Y. Liang Guan, K. Voon Ling, and C. Yuen, "Positioning with leo satellites as signals of opportunity (soop): A survey," *IEEE Transactions on Instrumentation and Measurement*, vol. 74, pp. 1–21, 2025.

[10] T. Maul, J. Robert, and S. Klob, "Ultra-precise synchronization for tdoa-based localization using signals of opportunity," in *2023 13th International Conference on Indoor Positioning and Indoor Navigation (IPIN)*, 2023, pp. 1–6.

[11] A. Coluccia, F. Ricciato, and G. Ricci, "Positioning based on signals of opportunity," *IEEE Communications Letters*, vol. 18, no. 2, pp. 356–359, 2014.

[12] H.-J. Shao, X.-P. Zhang, and Z. Wang, "Efficient closed-form algorithms for aoa based self-localization of sensor nodes using auxiliary variables," *IEEE Transactions on Signal Processing*, vol. 62, no. 10, pp. 2580–2594, 2014.

[13] A. Fascista, G. Ciccarese, A. Coluccia, and G. Ricci, "A localization algorithm based on v2i communications and aoa estimation," *IEEE Signal Processing Letters*, vol. 24, no. 1, pp. 126–130, 2017.

[14] K. Shamaei, J. Khalife, and Z. M. Kassas, "A joint toa and doa approach for positioning with lte signals," in *2018 IEEE/ION Position, Location and Navigation Symposium (PLANS)*, 2018, pp. 81–91.

[15] M. Orabi, J. Khalife, and Z. M. Kassas, "Opportunistic navigation with doppler measurements from iridium next and orbcomm leo satellites," in *Proceedings of IEEE Aerospace Conference*, 2021, pp. 1–9.
[16] S. E. Kozhaya and Z. M. Kassas, "Positioning with starlink leo satellites: A blind doppler spectral approach," in *2023 IEEE 97th Vehicular Technology Conference (VTC2023-Spring)*, 2023, pp. 1–5.
[17] P. Abouzar, D. G. Michelson, and M. Hamdi, "Rssi-based distributed self-localization for wireless sensor networks used in precision agriculture," *IEEE Transactions on Wireless Communications*, vol. 15, no. 10, pp. 6638–6650, 2016.
[18] S. R. Jondhale, R. Maheswar, and J. Lloret, *Received Signal Strength Based Target Localization and Tracking Using Wireless Sensor Networks*, 1st ed., ser. EAI/Springer Innovations in Communication and Computing. Springer Cham, 2021. [Online]. Available: https://doi.org/10.1007/978-3-030-74061-0
[19] J. He and H. C. So, "A hybrid tdoa-fingerprinting-based localization system for lte network," *IEEE Sensors Journal*, vol. 20, no. 22, pp. 13 653–13 665, 2020.
[20] Y. Zhang and K. C. Ho, "Localization by signals of opportunity in the absence of transmitter position," *IEEE Transactions on Signal Processing*, vol. 70, pp. 4602–4617, 2022.
[21] H. Jamali-Rad and G. Leus, "Sparsity-aware multi-source tdoa localization," *IEEE Transactions on Signal Processing*, vol. 61, no. 19, pp. 4874–4887, 2013.
[22] H. K. Dureppagari, C. Saha, H. S. Dhillon, and R. M. Buehrer, "Uav-based 5g localization for emergency response using signals of opportunity," in *2024 IEEE International Symposium on Dynamic Spectrum Access Networks (DySPAN)*, 2024, pp. 63–68.
[23] M. N. de Sousa, R. Sant'Ana, R. P. Fernandes, J. C. Duarte, J. A. Apolinário, and R. S. Thomä, "Improving the performance of a radio-frequency localization system in adverse outdoor applications," *EURASIP Journal on Wireless Communications and Networking*, vol. 2021, no. 1, p. 123, 2021. [Online]. Available: https://doi.org/10.1186/s13638-021-02001-6
[24] J. L. McGuire, Y. W. Law, K. Doğançay, S.-Y. Ho, and J. Chahl, "Optimal maneuvering for autonomous vehicle self-localization," *Entropy*, vol. 24, no. 8, 2022. [Online]. Available: https://www.mdpi.com/1099-4300/24/8/1169
[25] MathWorks, "fspl - free space path loss," https://nl.mathworks.com/help/comm/ref/fspl.html, 2026, accessed: 2026-06-20.
[26] Antennekaart.nl, "5g kaart van zendmasten in nederland," https://antennekaart.nl/kaart/5g, 2026, accessed: 2026-06-21.
[27] CellTowerMaps, "Cell towers near chicago, il," https://www.celltowermaps.com/cell-towers/near/city-state/chicago/il, 2026, accessed: 2026-06-21.
[28] MathWorks, "Raytracing - ray tracing propagation model," https://nl.mathworks.com/help/antenna/ref/rfprop.raytracing.html, 2026, accessed: 2026-06-20.
[29] ——, "raypl - path loss and phase change for rf propagation ray," https://nl.mathworks.com/help/antenna/ref/raypl.html, 2026, accessed: 2026-06-20.

APPENDIX

TABLE V: Key simulation parameters.

Parameter	Symbol	Open field	Urban (TU Delft)	Urban (Chicago)
Environment size	–	5000×5000 m	$\approx 1500 \times 1000$ m	$\approx 1000 \times 1000$ m
Number of transmitters	N_{tx}	6	7	8 / 20
Transmitter height (AGL)	–	15–60 m	4–42 m	6–282 m
Transmit power	P_{tx}	63 dBm	43 dBm	43 dBm
Carrier frequency	f_c	2.4 GHz	2.4 GHz	2.4 GHz
Propagation model	–	Friis FSPL (`fspl()`)	SBR ray tracing	SBR ray tracing
Max Reflections (swept)	–	–	2 / 4 / 8 / 16	2 / 4 / 8 / 16
Max Diffractions	–	–	1	1
RSSI shadow fading std	σ_{sf}	–	10	10
TDoA hardware timing noise std	σ_τ	10 ns	20 ns	20 ns
TDoA EKF NLOS spread std	σ_{NLOS}	–	100ns	100 ns
EKF RSSI path-loss exponent	n	–	3.2	3.8
EKF RSSI reference path loss	PL_0	–	40 dB	40 dB
EKF process noise covariance	$\mathbf{Q}$	$\text{diag}(5, 5, 5, 1, 1, 1)$	$\text{diag}(5, 5, 0.5, 1, 1, 0.1)$	$\text{diag}(5, 5, 0.5, 1, 1, 0.1)$
Fusion weight (TDoA)	w_τ	–	1.0	1.0
Fusion weight (RSSI)	w_{RSSI}	–	0.4	0.4
TDoA outlier std multiplier	γ	–	5	5
TDoA gate σ	σ	–	3	3
Time steps	T	200	30	30
Time step	Δt	1 s	2 s	2 s
Monte Carlo runs	N_{MC}	50	1	1

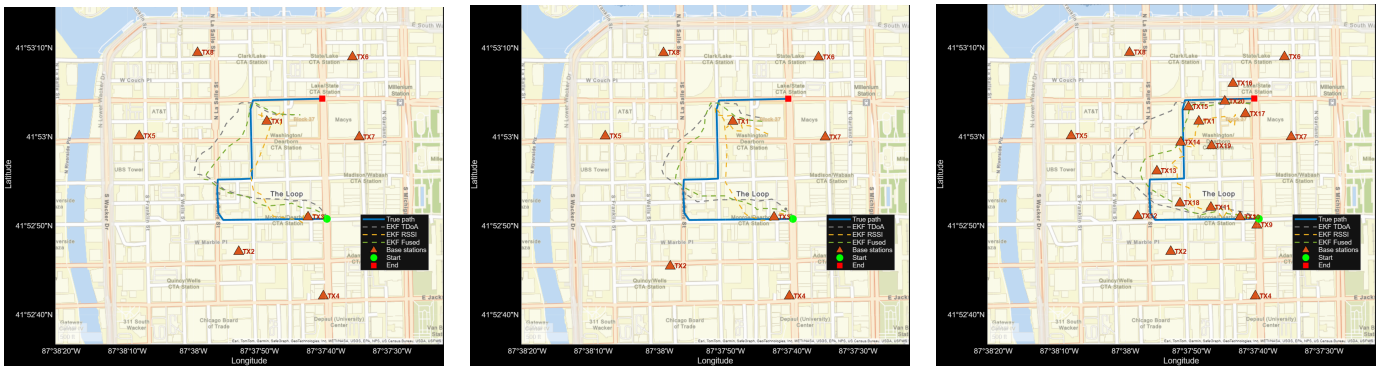

(a) TX2 LOS (164 m) (b) TX2 NLOS (44 m) (c) 20 TXs along trajectory

Fig. 3: Localization performance in the Urban Chicago scenario under different transmitter configurations.

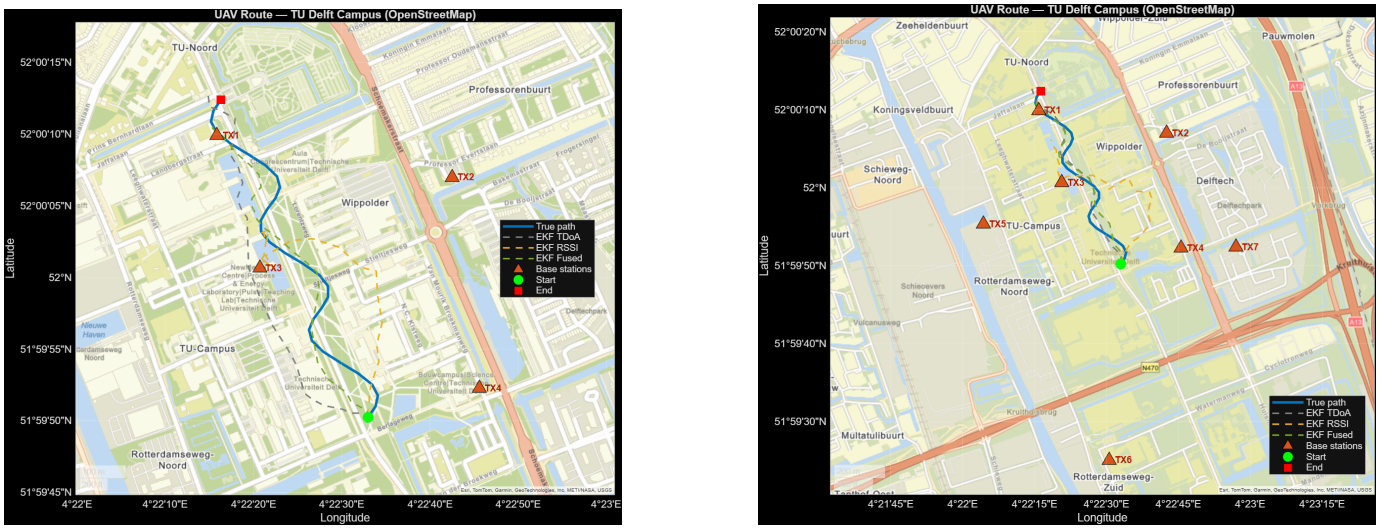

(a) 4 TX handpicked configuration (b) 7 TX real location configuration

Fig. 4: TU Delft scenario showing UAV route under different transmitter configurations (2 Reflections).